INTERNATIONAL JOURNAL OF RESEARCH IN PHARMACY AND CHEMISTRY

Available online at www.ijrpc.com

Research Article

SYNTHESIS AND CHARACTERIZATION OF INORGANIC POLYMER NANO – COMPOSITES FROM METHYL ACRYLATE AND ALUMINUM CHLORIDE AND HEXACHLORO PALATINATE (IV)

Nada M. Abbass and Safaa Zamel*

Department of Chemistry, College of Science, University of Baghdad, Iraq.

ABSTRACT

The polymer nanocomposites (a) AL_2O_3 Fe_2O_4 (b) $PtO_2Fe_2O_4$ were synthesized by ferric chloride target metal salts and methyl acrylate aqueous solution 1:2 molar ratio with stirring. FTIR, x-ray diffraction (XRD), atomic force microcopy (AFM), thermogravimetric analysis (TG of DTG) and differential scanning calorimetry (DSC) were employed to character the resultant nanocomposites. The results of XRD and AFM showed that the nanocomposites were a hybrid of the polymer and the metal oxides nanoparticles which were distributed uniformly in general. The FTIR spectra of oxides (a and b) appeared in the rang 465-611 cm^{-1} which shows the formation of a single phase spinal structure having two sub lattices, tetrahedral and octahedral sites. Two peaks appear in the range of 1369-1398 cm^{-1} are due to C-O stretching by anhydride group in the metal oxides, emphasizes the methylacrylate formed as polymer with spinal oxide. The (TG of DTG) analysis gave an indication of the thermal dissociation nature of the inorganic nanocomposites at high temperatures. DSC characterization of nanocomposites materials showed the effect of fillers on the crystallization behavior of the pure methyl acrylate. The corrosion resistance in saline water (3.5 % NaCl) at 293 K were studied.

Keywords: Polymer composites, methyl acrylate, aluminum chloride, corrosion, XRD.

INTRODUCTION

The purpose of the preparation of the "nanocomposite" is to obtain the synergic effect of the polymer and the inorganic compound. Nanocomposites have strange structure, a phase separated structure, with a nanoscale interface between the polymer matrix and the inorganic compound (nanophase separated structure)[1]. Polymernanocomposite is apolymer or a"co-Polymer" having dispersed in its Nano particles[2]. The coordination polymers are also important for synthesizing the inorganic polymer nanocomposites[3], which exhibit eminent mechanical characteristics, heat resistance and chemical resistance compared to the heat or traditionally filled resins[4]. Polymer composites containing ferrites are increasing replacing the classical ceramic magnetic materials because of their mouldability and reduction in cast[5,6,7]. The synthesis of polymer nanocomposites is a complete aspect of polymer nano technology by introduce the nano metric inorganic compounds[8]. Tania Ribeiro and J.Farinha reported that the hybrid organic/inorganic materials combine the rigidity and high thermal stability of the inorganic material with flexibility, ductility and process ability of the organic polymers[9].

MATERIALS AND METHODS

Materials and measurement

The chemical reagents, $FeCl_3.6H_2O$, $Al\ Cl_3.6H_2O$, H_2PtCl_6, $(NH_4)_2\ S_2O_8$, methyl acrylate and NaOH were used as obtained. Without further purifications, all reagents were used which are analytical grade.

Preparation of standard solution

A aqueous solution of methyl acrylate (methyl acrylate: water: 3:1) and 5%, ammonium per sulphate solution were prepared for experiment. The standard solution was prepared by dissolving stoichiometric amounts of the metal salts in distilled water. The sodium hydroxide solution was standardized against a solution of oxalic acid as a primary standard solution and it was titrated as dibasic acide. 25 ml of oxalic acid and 8 drops of phenolphthalein was titrated with the NaOH solution, often neutralized of all the acid, a more stable pink color was appeared, stirred often addition of the last drop of NaOH.

Synthesis of complexes

The complexes were prepared according to a method described by B.P.Singh[10] Scheme (1) illustrates the preparation of the polymer nanocomposites

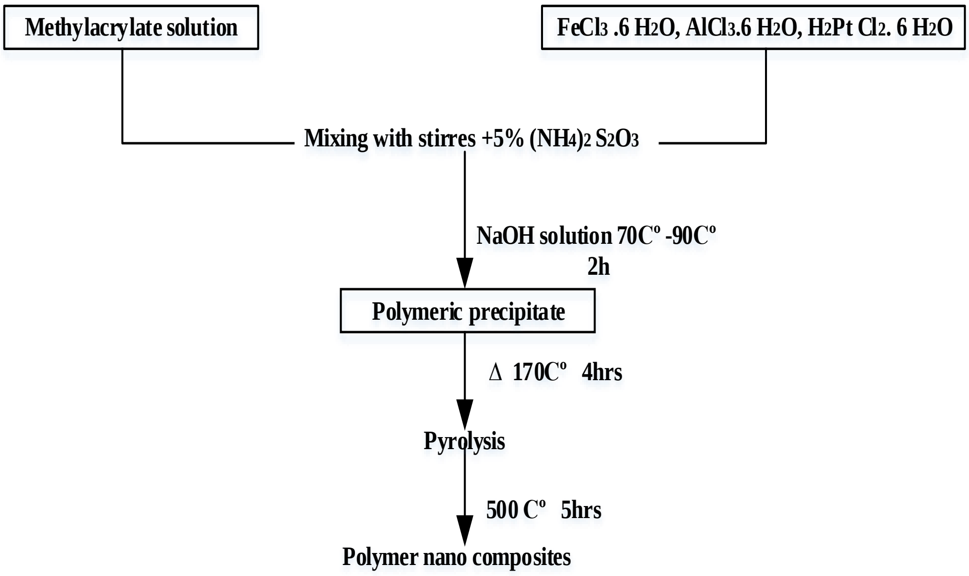

Scheme. 1: Prepartion rote of polymer nanocomposite

Ferric chloride solution (10 ml, 0.1 N) were added to 10 ml of methyl acrylate solution (methyl acrylate: water:7:3) with stirring. At 70-90 °C, 5%$(NH_4)_2S_2O_8$ (5ml) added to the above solution for two hours. The solution were dried to yield the poly methyl acrylate which were dried at 90-100°C ever night and were heated at 170 °C about 4 hours to obtained the amorphous nature of salt. The last salts were heated at 500 °C for five hours in air, quietly cooled and collected.

FI-IR spectroscopy

The FI-IR (fig. 1 and 2) of compounds a, b offered the ν_{c-c} andν_{c-o}stretching were certain due to the aspect of peaks at 1369 – 1398 cm^{-1}, promoted the anhydride group of methyl acrylate ready in compounds (a +b) as polymeric from. The bands in the region 465-611 cm^{-1} particular the formation of single phase spinal structures[11].

Table 1: FT-IR spectra of compounds

Compounds	Wave numbers of absorption band ν (cm^{-1})			
	$\nu\,(c-o)$	$\nu\ c-c$	Single phase spinal structure	
			ν_4	ν_5
AL Fe_2O_4	1369	1425	611	465
Pt Fe_2O_4	1398	1425	619	457

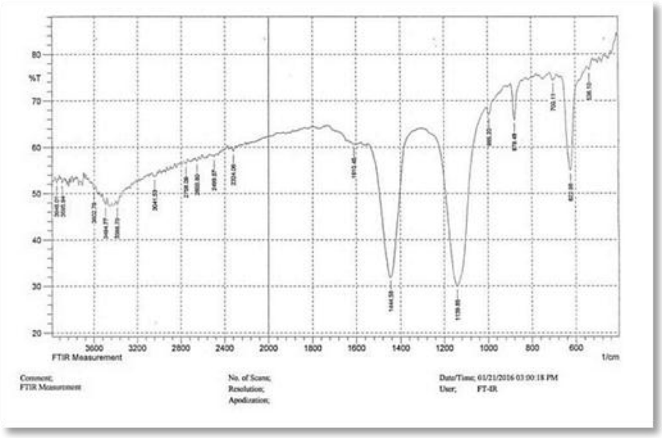

Fig.1: FT-IR spectra of compound (a)

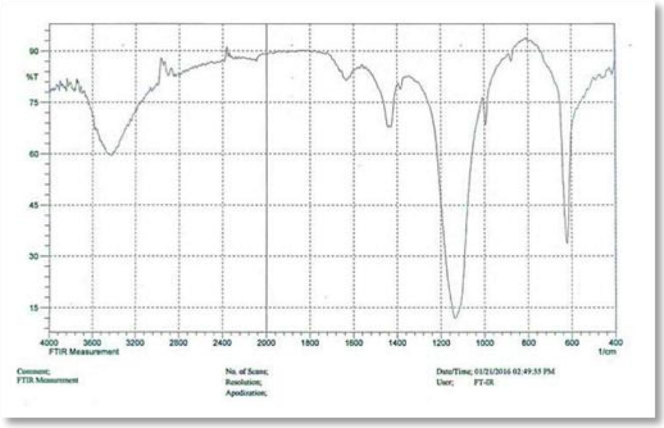

Fig.2: FT-IR spectra of compound (b)

Thermal properties of a + b nanocomposites (DSC)

Based on experimented data executed by authors[12], nanocompositesa+bwere investigated. As illustrated (figure 3 and 4), the glass transition region exist over a temperature rang. Consequently, Tg located as the point of bending of the DSC curve at 82, 95 C° for (a and b) CompositesRespectively. The melting temperature and expand of crystalling were spotted to be constrained by the change in the filler surface modification, this ticked that under the condition utilized for synthesis of the composites[13], the modified filler had no impact on the crystallinity of the filler of nanocomposite (a)[14]. The DSC of thermogram of nanocomposite (b) showed a forward crystallization and a fibrous morphology rather than (Al PMA) or nanocomposite a, behavior.

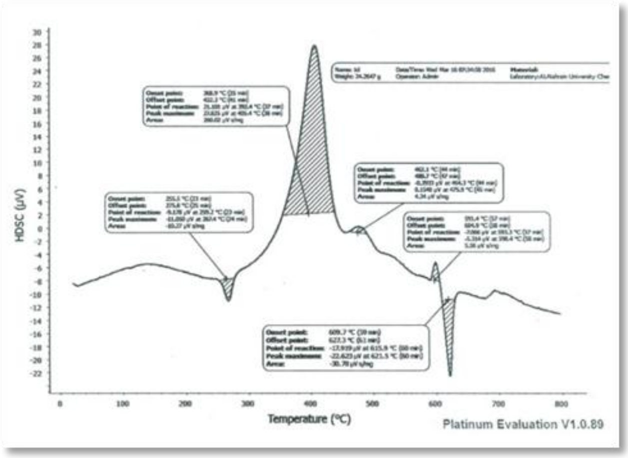

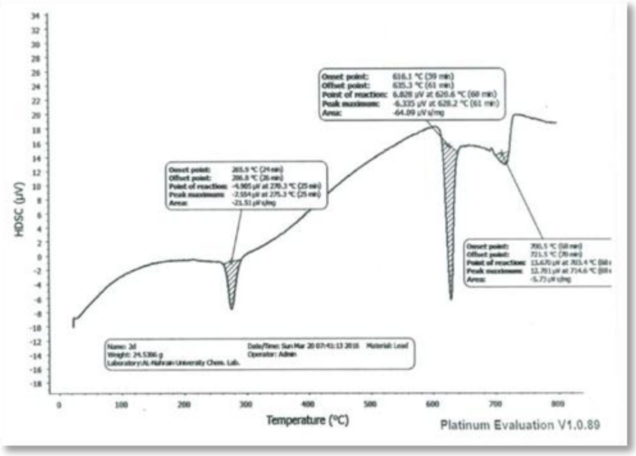

Fig. 3: DSC curve of compound (a)

Fig. 4: DSC curve of compound (b)

Surface of Polymer – Metal oxide nanocomposite

The surface of the Al, polymer (a) and Pt, polymers (b), were spotted with atomic Microscope (AFM) fig (5 and 6). The image of AFM exhibited that the surface of the polymer brush was very soft because it contained polymer chins that had the same rise.

It is notion that the holes are formed by oxygen evolution taking place during the oxidation process. Surface of the Nano oxides layers were soft and did not show any divergence in height by more than 6 nm figuresshow the topographic structures in 2 D and 3D vision of AFM images of (a and b) nanocomposites layers builded on stainless steel specimen[15, 16]

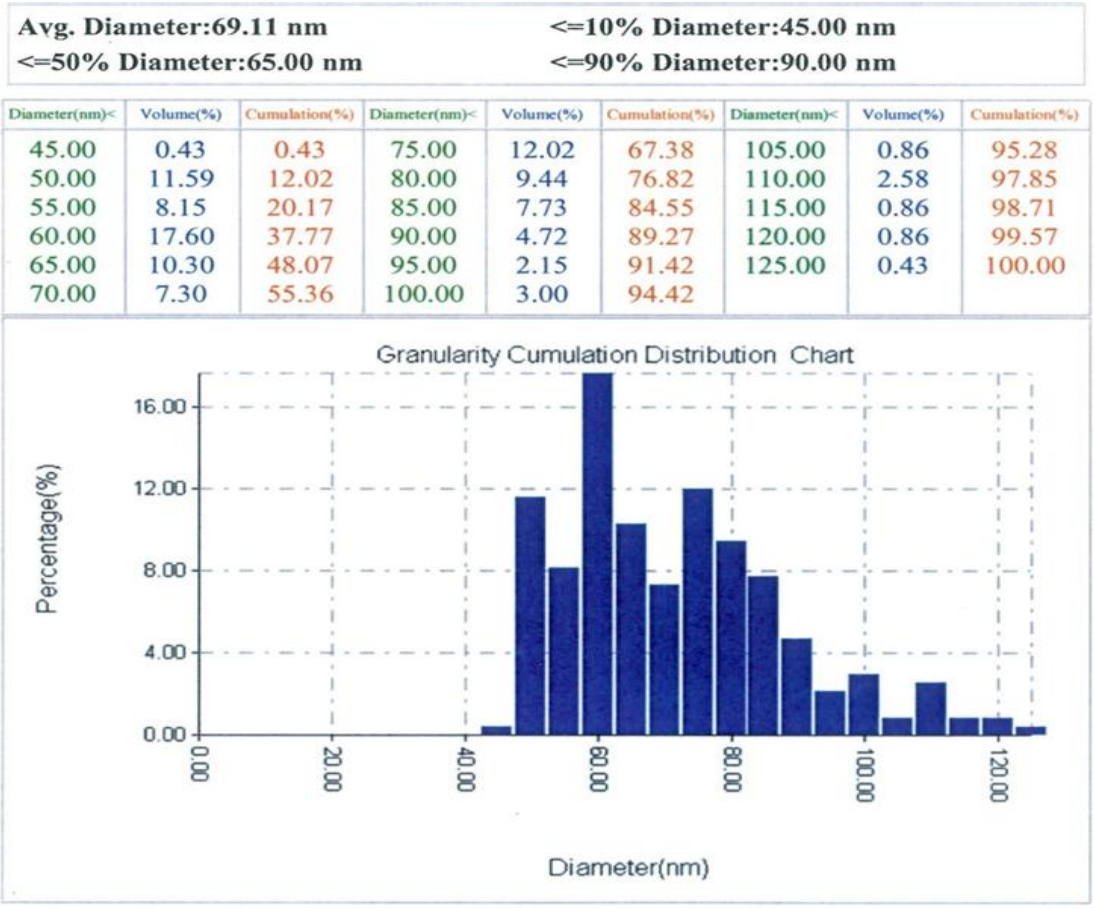

Avg. Diameter:69.11 nm **<=10% Diameter:45.00 nm**
<=50% Diameter:65.00 nm **<=90% Diameter:90.00 nm**

Diameter(nm)<	Volume(%)	Cumulation(%)	Diameter(nm)<	Volume(%)	Cumulation(%)	Diameter(nm)<	Volume(%)	Cumulation(%)
45.00	0.43	0.43	75.00	12.02	67.38	105.00	0.86	95.28
50.00	11.59	12.02	80.00	9.44	76.82	110.00	2.58	97.85
55.00	8.15	20.17	85.00	7.73	84.55	115.00	0.86	98.71
60.00	17.60	37.77	90.00	4.72	89.27	120.00	0.86	99.57
65.00	10.30	48.07	95.00	2.15	91.42	125.00	0.43	100.00
70.00	7.30	55.36	100.00	3.00	94.42			

Fig. 5: The reprint of AFM reports for statistical measuring particle size and their distributions of nanometaloxides / polymer layers on SS 316 specimen

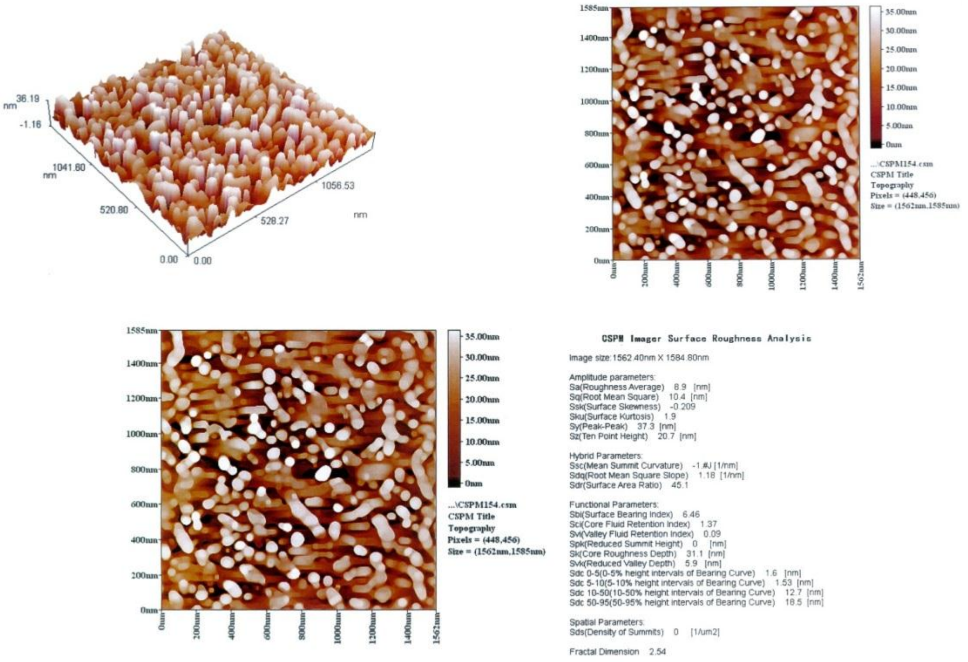

CSPM Imager Surface Roughness Analysis

Image size:1562.40nm X 1584.80nm

Amplitude parameters:
Sa(Roughness Average) 8.9 [nm]
Sq(Root Mean Square) 10.4 [nm]
Ssk(Surface Skewness) -0.209
Sku(Surface Kurtosis) 1.9
Sy(Peak-Peak) 37.3 [nm]
Sz(Ten Point Height) 20.7 [nm]

Hybrid Parameters:
Ssc(Mean Summit Curvature) -1.#J [1/nm]
Sdq(Root Mean Square Slope) 1.18 [1/nm]
Sdr(Surface Area Ratio) 45.1

Functional Parameters:
Sbi(Surface Bearing Index) 6.46
Sci(Core Fluid Retention Index) 1.37
Svi(Valley Fluid Retention Index) 0.09
Spk(Reduced Summit Height) 0 [nm]
Sk(Core Roughness Depth) 31.1 [nm]
Svk(Reduced Valley Depth) 5.9 [nm]
Sdc 0-5(0-5% height intervals of Bearing Curve) 1.6 [nm]
Sdc 5-10(5-10% height intervals of Bearing Curve) 1.53 [nm]
Sdc 10-50(10-50% height intervals of Bearing Curve) 12.7 [nm]
Sdc 50-95(50-95% height intervals of Bearing Curve) 18.5 [nm]

Spatial Parameters:
Sds(Density of Summits) 0 [1/um2]

Fractal Dimension 2.54

Fig. 6: 2 D and 3D vision of AFM images of (a) nanocomposites layers builded on stainless steel specimen

Avg. Diameter:87.30 nm

Diameter(nm)<	Volume (%)	Cumulation(%)	Diameter(nm)<	Volume (%)	Cumulation(%)	Diameter(nm)<	Volume (%)	Cumulation(%)
40.00	2.56	2.56	70.00	5.13	19.66	100.00	10.26	68.38
45.00	1.71	4.27	75.00	10.26	29.91	105.00	9.40	77.78
50.00	1.71	5.98	80.00	5.98	35.90	110.00	7.69	85.47
55.00	2.56	8.55	85.00	5.13	41.03	115.00	6.84	92.31
60.00	2.56	11.11	90.00	11.11	52.14	120.00	5.13	97.44
65.00	3.42	14.53	95.00	5.98	58.12	125.00	2.56	100.00

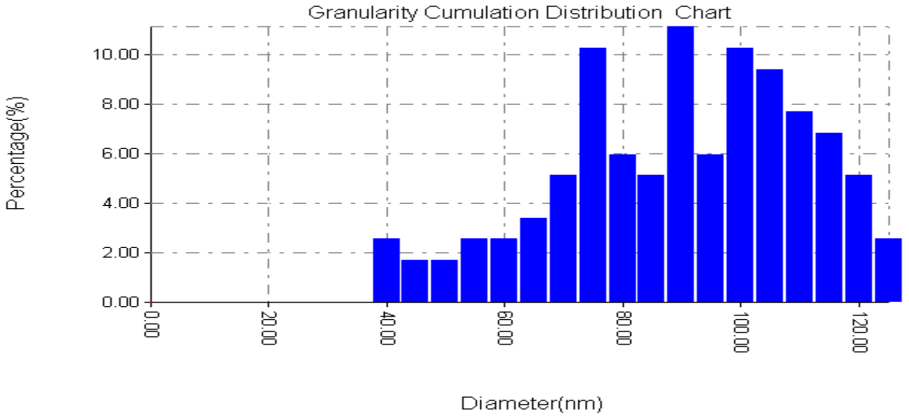

Fig. 7: The reprint of AFM reports for statistical measuring particle size and their distributions of nanometaloxides / polymer layers on SS 316 specimen

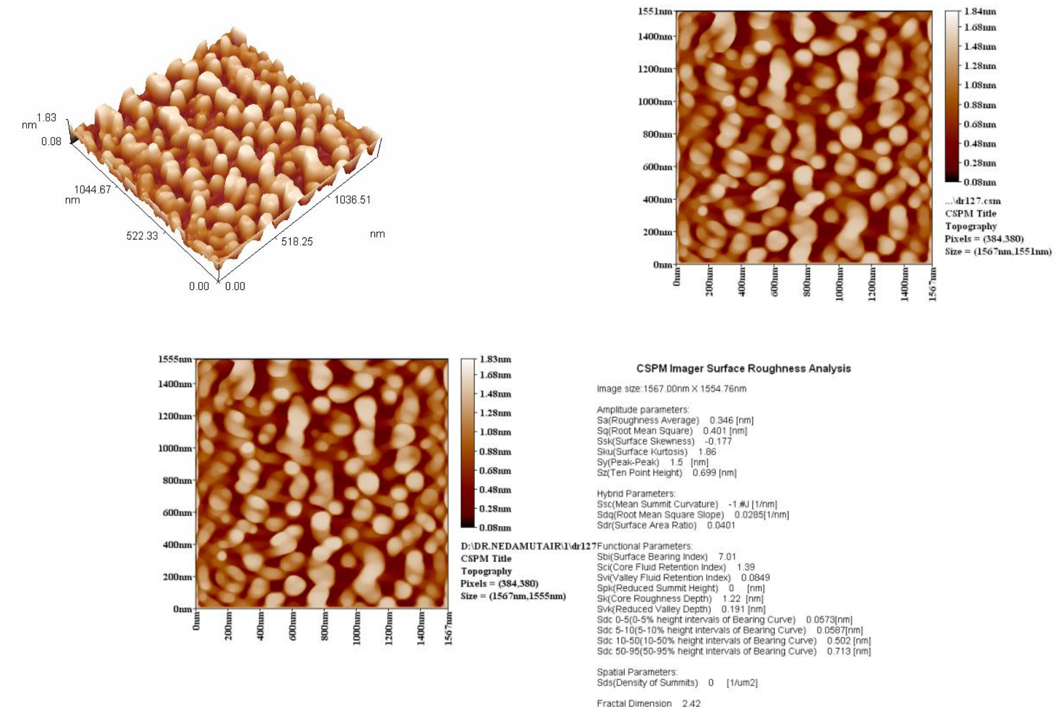

CSPM Imager Surface Roughness Analysis

Image size:1567.00nm X 1554.76nm

Amplitude parameters:
Sa(Roughness Average) 0.346 [nm]
Sq(Root Mean Square) 0.401 [nm]
Ssk(Surface Skewness) -0.177
Sku(Surface Kurtosis) 1.86
Sy(Peak-Peak) 1.5 [nm]
Sz(Ten Point Height) 0.699 [nm]

Hybrid Parameters:
Ssc(Mean Summit Curvature) -1.#J [1/nm]
Sdq(Root Mean Square Slope) 0.0285[1/nm]
Sdr(Surface Area Ratio) 0.0401

Functional Parameters:
Sbi(Surface Bearing Index) 7.01
Sci(Core Fluid Retention Index) 1.39
Svi(Valley Fluid Retention Index) 0.0849
Spk(Reduced Summit Height) 0 [nm]
Sk(Core Roughness Depth) 1.22 [nm]
Svk(Reduced Valley Depth) 0.191 [nm]
Sdc 0-5(0-5% height intervals of Bearing Curve) 0.0573[nm]
Sdc 5-10(5-10% height intervals of Bearing Curve) 0.0587[nm]
Sdc 10-50(10-50% height intervals of Bearing Curve) 0.502 [nm]
Sdc 50-95(50-95% height intervals of Bearing Curve) 0.713 [nm]

Spatial Parameters:
Sds(Density of Summits) 0 [1/um2]

Fractal Dimension 2.42

Fig. 8: 2 D and 3D vision of AFM images of (b) nanocomposites layers builded on stainless steel specimen

X -ray diffraction pattern

The X -ray diffraction patterns of compounds a and b shows in figure (9 and 10) respectively and are presented data of crystalline information several diffraction peaks in a (AL / PMA) patterns at 2$^{\theta}$ = 18.2°, 32.1° , 34.2°, 45.5° , 48.0° and 57.2° were recorded, and peaks at 2$^{\theta}$ = 19.1° , 31.9° , 39.9° , 45.5° and 46.5° were registered in the XRD pattern of modified b (Pt / PMA), inclusion the presence of the order structure of (a and b). it showed that these oxides crystallizes in a cubic crystal. The two oxides display spinal structures in the XRD patterns. Using (scherer'sequation)in table (2).

Table 2: The unit cell dimensions of compounds at 500C$^{\circ}$.

Compounds	Particle size / AFM (nm) (avg.)	Crystal size nm
Al Fe_2O_4	69.11	26.65
Pt Fe_2O_4	87.71	31.71

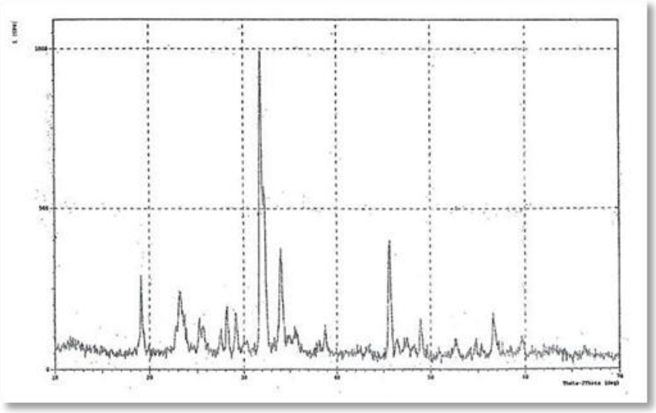

Fig.9: XRD of compound (a)

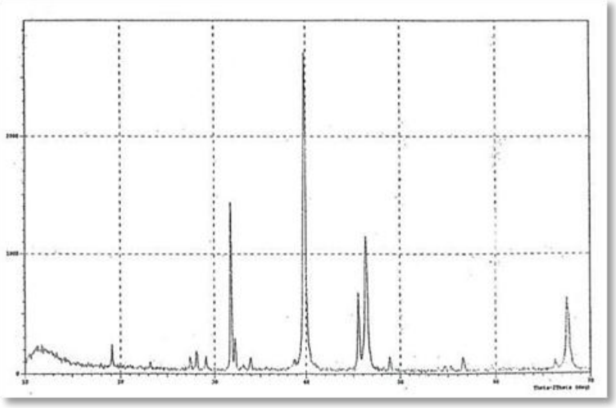

Fig.10: XRD of compound (b)

Thermogravimetric analysis TG of DTG

Thermal analysis of (a and b) nanocomposites were given in figures (11 and 12) respectively. Les 100 C° , the weight decreases originate from moisture inside sample (water). The thermal behavior of the nanocomposites in TG of DTG thermaograms shows a coherence between the composite compounds and thermal degradation of the composites begins at a higher temperature (610-897Cº) attributed to the highthermal decomposition of the composites[17.18] in the table (3 and 4).

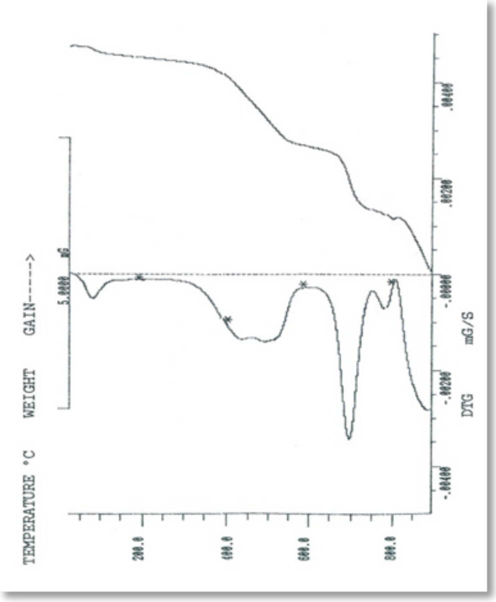

Fig. 11:TG and DTG curve & compound(a)

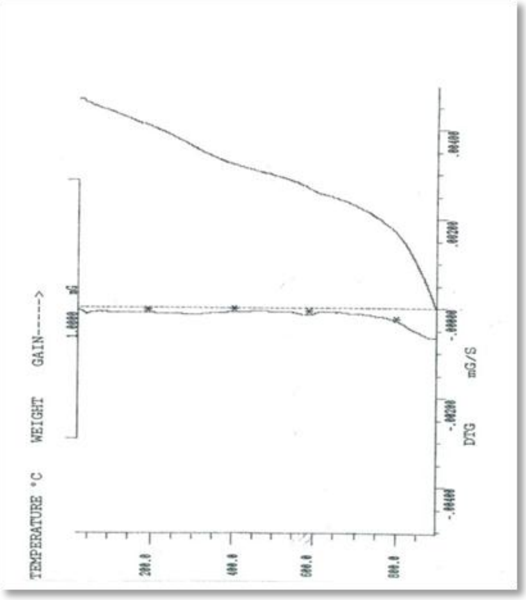

Fig. 12:TG and DTG curve & compound(b)

Table 3: Thermal decomposition of compsite(a)

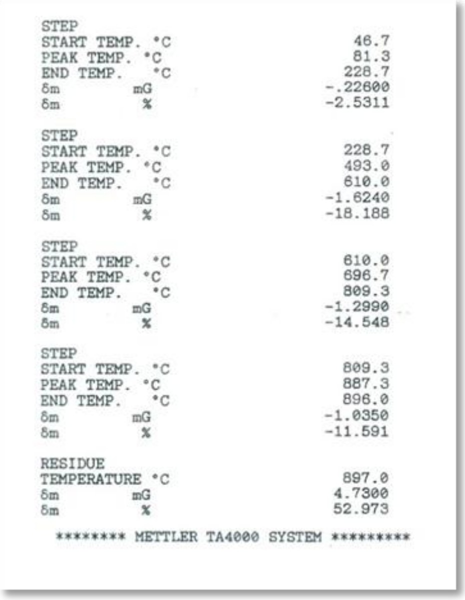

```
STEP
START TEMP. °C                 46.7
PEAK TEMP. °C                  81.3
END TEMP.   °C                228.7
δm          mG              -.22600
δm           %              -2.5311

STEP
START TEMP. °C                228.7
PEAK TEMP. °C                 493.0
END TEMP.   °C                610.0
δm          mG              -1.6240
δm           %              -18.188

STEP
START TEMP. °C                610.0
PEAK TEMP. °C                 696.7
END TEMP.   °C                809.3
δm          mG              -1.2990
δm           %              -14.548

STEP
START TEMP. °C                809.3
PEAK TEMP. °C                 887.3
END TEMP.   °C                896.0
δm          mG              -1.0350
δm           %              -11.591

RESIDUE
TEMPERATURE °C                897.0
δm          mG               4.7300
δm           %               52.973

******** METTLER TA4000 SYSTEM *********
```

Table 4: Thermal decomposition ofcompsite(b)

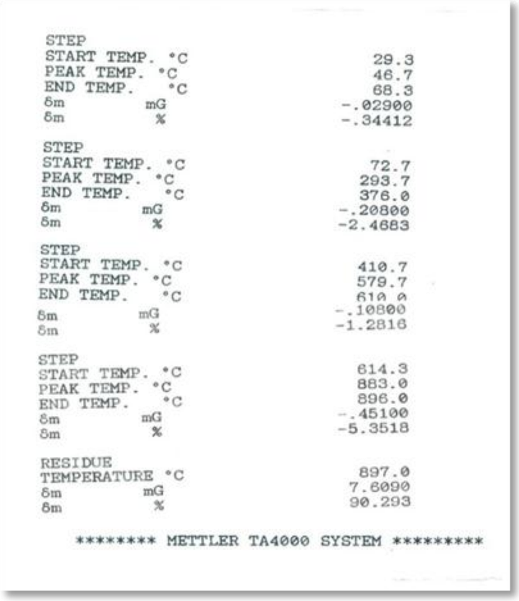

```
STEP
START TEMP. °C                 29.3
PEAK TEMP. °C                  46.7
END TEMP.   °C                 68.3
δm          mG              -.02900
δm           %              -.34412

STEP
START TEMP. °C                 72.7
PEAK TEMP. °C                 293.7
END TEMP.   °C                376.0
δm          mG              -.20800
δm           %              -2.4683

STEP
START TEMP. °C                410.7
PEAK TEMP. °C                 579.7
END TEMP.   °C                610.0
δm          mG              -.10800
δm           %              -1.2816

STEP
START TEMP. °C                614.3
PEAK TEMP. °C                 883.0
END TEMP.   °C                896.0
δm          mG              -.45100
δm           %              -5.3518

RESIDUE
TEMPERATURE °C                897.0
δm          mG               7.6090
δm           %               90.293

******** METTLER TA4000 SYSTEM *********
```

Corrosion measurement estimation

Electrochemical corrosion kinetics of compounds (a and b) were characterized by maint three polarization parameters encompasses, corrosion current density (I_{corr}), corrosion potential (E_{corr}) and tafel slopes, anodic region (βa) and cathodic region (βc), by a polarization curve ($E_{vs.i}$) and the corrosion rate[19]. The above parameters accordions to the following eq. are given in table (5).

$$R_b = \frac{B}{i_{corr}} \textbf{where}$$

$$B = \frac{B_a B_c}{2.303\,(B_a + B_c)}$$

$$\textbf{PE \% =} \left[1 - \frac{i_{corr}}{\dot{i}_{corr}}\right] \textbf{ where PE\% is the inhibition efficiency}$$

i_{corr}andi_{corr} are the corrosion current densities of uncoated and coated speciments respectively.

AL. Fe_2O_4 / PMA and Pt, Fe_2O_4 / PMA) / carbon steel in salin water (3.5% NaCl) system.

The potentiodynamic polarization curves of CS specimens beneath realization without and with nanocomposites and b coating immersed in sea water at 293 k, are illustrate in figure (13 and 14) of uncoated and coated carbon steel fornanocomposites a and b respectively.

The shift in Ecorr of the coated nanocaposites with comparison of the uncoated sample was show in tabel (5)corrosion measurements parameters for uncouted and coated carbon steel (CS) with non compositespecimens in 3.5% NaCl at 298k.

The results indicates the corrosion resistant advantage of the coating, as well it observed that the values of corrosion current density (icorr) for nano composites coated CS are lower than corresponding values for bare CS. The PE% of coated samples explains the effect of coating process and the better protection ability for CS metal at 298k.[20]

Table 5: corresion measurement paramerters for coated &uncoated carbon steel specimens in 3.5%NaCl at 293ºC

T(K)		E_{corr} (mV)	i_{corr} (μA/cm^2)	/Bc/ (mV/Dec)	/Ba/ (mV/Dec)	R_p Ω.cm^2	CR (gm/m^2.d)	CP (mm/y)	PE%	ρ%
Uncoated CS	293	-415.8	48.86	138.8	107.7	532.1	12.2	0.567	-	-
coated CS with methyl acrylate + Al^{+3}	293	-217.4	16.08	119.9	129.4	1679.1	4.02	0.187	67.1	0.44
coated CS with methyl acrylate + pt^{+4}	293	-189.6	20.60	114.2	100.5	1116.5	5.15	0.239	57.8	0.37

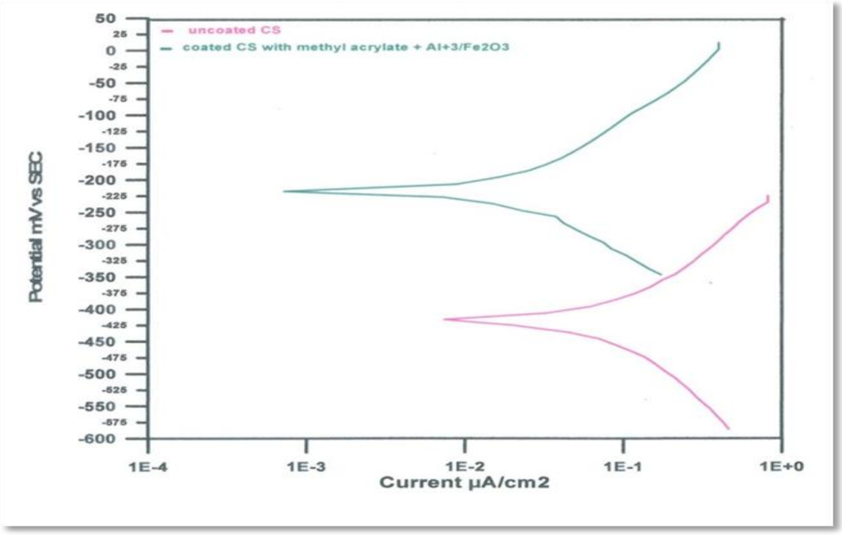

Fig. 13: Tafle plots of uncoated & coated *SS*316 in 3.5NacI of compound(a)

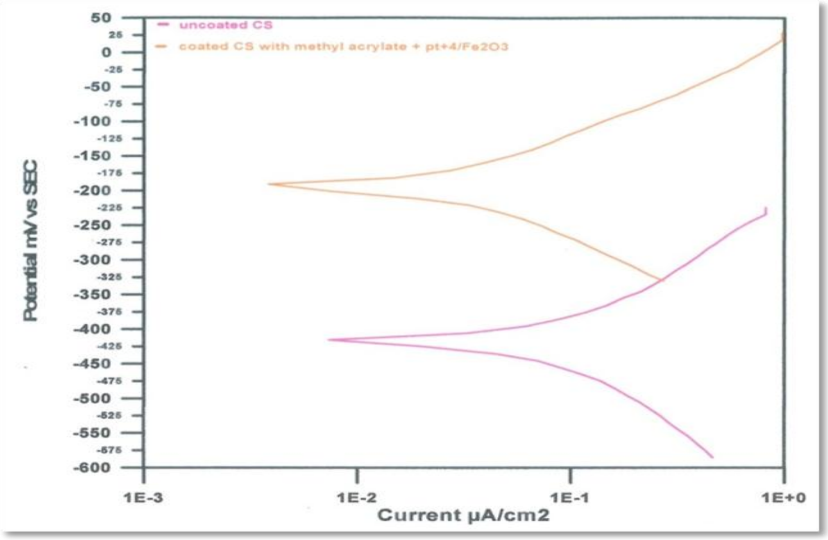

Fig. 14: Tafle plots of uncoated & coated *SS*316 in 3.5NaCl of compound (b)

CONCLUSION

The nanocomposites were prepared by the react of ferric chloride, metal chlorides and metly acrylate. FT-IR analysis exhibited that the metlylacrylate polymerizes at low temperature and composes spinal ferrite. The study of XRD powder pattern and AFM images composes spinal crystal with crystalline size in the range of 26-30 nm with partical size of 69-87nm. Both DSC and TG indicated if there is presence of any excess of surface modification molecules existing as pseudo bilayer , but unbound to the polymers surface, the twonanocomposites (a and b) coated metals under investigation undergoes increasing of the corrosion protection properties at 293 k.

REFERENCES

1. K Nam, Y Tsutsumi and C Yoshikawa. Preparation of novel polymer- metal oxide nanocomposites with nanophaseseparalhierarchied structure. Bull Mater Sci. 2011;34(7): 1289-1296.
2. Vargo TG, Koloski TS and Macrae DM. Novel Nano- Metal polymeric composites Fabricated via In- situ self A ssembly, NSTI- Nanotech. 2006;2:772-777.
3. Vikas Mittal. Play Nanocomposites: Synthesis, Microstructure, and properties. Copyright.
4. Yu J, Lin RYF, poon B, Nazarenko S, Koloki TS, Vargo TG, Baer E and Hiltner A. Polymers with palladium Nano-particles as Active Membrane Materials. J Appl Polym Sci. 2004;92:749.
5. Gubin SP, koksharov YU, Khomutov A and YurkovG YU. Magnetic nanoparticles: preparation, structure and properties. Russian chemical Reviews. 2005;74:489-520.
6. Lau CMY. A stady of blending and complexation of polycacrylic acid poly (vinyl Ryrrolidone), Polymer. 2002;43(3):823-829.
7. Bashar Issa, ihad M obaidat and yousefhaik. Magnatic Nanoparticles :surface effect andproperties Related to Biomedicine Applications. Int J MOL Sci. 2013;14(11):21266-21305.
8. Vargo TG, Koloski TS and Brupbacher JB. Novel Nano-metal polymeric composites Fabricated via In- situ self Assembly. www.nsti. Org, ISBN 0-9767985-7-3. 2006;2.
9. Tania Ribriro and Farinha T. Functional Functional Films from silica/ pohymen Nanoparticles," Materials. 2014;7:3881-3900.
10. Birendrap Singh, Jai P Singh and Shruti S. Synthesis and characterization of Inorganic polymen Nano- Composites. Der chemicasinica. 2012;3(2):521-526.
11. Sanchez C, Julian B and Belleville. Applications of hybrid organic-inorganic nanocomposites, J Mate Chem. 2005;15:3559–3592.
12. Jone M Barton. The application of differential scanning calorimetry (DSC) to the study of epoxy resinins curing reaction. 2004;27:111-154.
13. Vikas M. Polymelnanocomposites: sythesis, microstruture, and properties. copyright © wiley – VCH verlageGmb H & Co. KGaA, Weinheim ISBN: 978-3-527-32521-4. 2010.
14. Nam K, Tsutsumi Y, Yoshikawa C and others. Preparation of novel polymen – metal oxide nanocomposites with nanophase separated hierarchical structure. bull Mates Sa. 2011;34(7): 1289-1296.
15. Oliveira M, Moraes J and Faez R. Impedance studies of poly methyl methacrylate – co - acrylic acide) doped polyanilinelilns on aluminum alloy. Progress in organic coatings. 65(3): 348-356.
16. Yuan XY, Zou LL and Liao CC. Improved properties of chemically modified graphene / poly methyl methacrylate) nanocomposites via a facile in – situ bulk polymerization. Express polymer letters. 2012;6(10):847–858.
17. Panl DR and Robeson LM. Polymer nanotechnology: nanocomposites, polymer. 2008;49:3187-3204.
18. Ale KsandraTurkovic. Metal oxide nano- particles and nano-composite polymen electrolytes – electrodes and electrolytes in solas and galvanic cells of the second generation, Actachimicaslovenica. 2008:55(4):822-827.
19. Bing Xue, YinshamJian and Darui Liu. Preparation and characterization of a Novel Anticorrosion Material, Materials Transactions. 2011;52(1):96-101.
20. Uhliy HH and Revie RW. Uhlig's corrosion handbook. Val.51: John Wiley of sons, 2011.